Atmos. Chem. Phys., 13, 2031–2044, 2013
www.atmos-chem-phys.net/13/2031/2013/
doi:10.5194/acp-13-2031-2013

Atmospheric Chemistry and Physics Open Access

Evaluation of HO_x sources and cycling using measurement-constrained model calculations in a 2-methyl-3-butene-2-ol (MBO) and monoterpene (MT) dominated ecosystem

S. Kim[1,a], G. M. Wolfe[2,b,c], L. Mauldin[1,d,e], C. Cantrell[1], A. Guenther[1], T. Karl[1], A. Turnipseed[1], J. Greenberg[1], S. R. Hall[1], K. Ullmann[1], E. Apel[1], R. Hornbrook[1], Y. Kajii[3,f], Y. Nakashima[3,g], F. N. Keutsch[2], J. P. DiGangi[2], S. B. Henry[2], L. Kaser[4], R. Schnitzhofer[4], M. Graus[5,6], A. Hansel[4], W. Zheng[1], and F. F. Flocke[1]

[1]ACD/NESL/NCAR Boulder, CO 80301, USA
[2]Department of Chemistry, University of Wisconsin, Madison, WI, USA
[3]Division of Applied Chemistry, Tokyo Metropolitan University, Tokyo
[4]University of Innsbruck, Innsbruck, Austria
[5]CIRES, University of Colorado, Boulder, CO 80309 USA
[6]Chemical Science Division, ESRL-NOAA, Boulder, CO 80305, USA
[a]now at: Department of Earth System Science, University of California, Irvine, CA, USA
[b]now at: Joint Center for Earth Systems Technology, Baltimore County, MD USA
[c]now at: NASA Goddard Space Flight Center, Greenbelt, MD, USA
[d]now at: Department of Physics, University of Helsinki, Helsinki, Finland
[e]now at: Department of Atmospheric and Oceanic Sciences, University of Colorado, Boulder, CO, USA
[f]now at: Graduate School of Environmental Studies and Human and Environmental Studies, Kyoto University, Kyoto, Japan
[g]now at: Department of Environmental and Natural Resource Sciences, Tokyo University of Agriculture and Technology, Tokyo, Japan

Correspondence to: S. Kim (saewungk@uci.edu)

Received: 8 April 2012 – Published in Atmos. Chem. Phys. Discuss.: 27 June 2012
Revised: 13 December 2012 – Accepted: 7 January 2013 – Published: 21 February 2013

Abstract. We present a detailed analysis of OH observations from the BEACHON (Bio-hydro-atmosphere interactions of Energy, Aerosols, Carbon, H_2O, Organics and Nitrogen)-ROCS (Rocky Mountain Organic Carbon Study) 2010 field campaign at the Manitou Forest Observatory (MFO), which is a 2-methyl-3-butene-2-ol (MBO) and monoterpene (MT) dominated forest environment. A comprehensive suite of measurements was used to constrain primary production of OH via ozone photolysis, OH recycling from HO_2, and OH chemical loss rates, in order to estimate the steady-state concentration of OH. In addition, the University of Washington Chemical Model (UWCM) was used to evaluate the performance of a near-explicit chemical mechanism. The diurnal cycle in OH from the steady-state calculations is in good agreement with measurement. A comparison between the photolytic production rates and the recycling rates from the $HO_2 + NO$ reaction shows that recycling rates are ~20 times faster than the photolytic OH production rates from ozone. Thus, we find that direct measurement of the recycling rates and the OH loss rates can provide accurate predictions of OH concentrations. More importantly, we also conclude that a conventional OH recycling pathway ($HO_2 + NO$) can explain the observed OH levels in this non-isoprene environment. This is in contrast to observations in isoprene-dominated regions, where investigators have observed significant underestimation of OH and have speculated that unknown sources of OH are responsible. The highly-constrained UWCM calculation under-predicts observed HO_2 by as much as a factor of 8. As HO_2 maintains oxidation capacity by recycling to OH, UWCM underestimates observed OH by as much as

a factor of 4. When the UWCM calculation is constrained by measured HO_2, model calculated OH is in better agreement with the observed OH levels. Conversely, constraining the model to observed OH only slightly reduces the model-measurement HO_2 discrepancy, implying unknown HO_2 sources. These findings demonstrate the importance of constraining the inputs to, and recycling within, the RO_x radical pool ($OH + HO_2 + RO_2$).

1 Introduction

Since Levy (1971) first postulated tropospheric OH production, recycling, and loss mechanisms, one of the main research topics in tropospheric photochemistry has been assessing OH concentrations in the troposphere due to its significance in determining lifetimes of most trace gases including methane, an important greenhouse gas. Concentrations of very reactive (short-lived) species like OH are usually reasonably well predicted by pseudo-steady state calculations. However, early model results (Levy, 1972; Wofsy et al., 1972; Crutzen, 1974) indicated significant discrepancies for global mean OH concentrations derived from atmospheric CH_3CCl_3 concentrations (Singh, 1977; Lovelock, 1977). Therefore, early modeling studies highlighted the need for development of a comprehensive understanding of ozone-CO-CH_4-NO_x ($NO + NO_2$) chemistry to resolve these discrepancies (Logan et al., 1981). Although Logan et al. (1981) acknowledged that reactive biogenic volatile organic compounds (BVOCs) such as isoprene and monoterpenes (MT) could significantly depress local concentrations of OH, Chameides and Cicerone (1978) argued that non-methane hydrocarbons (NMHC) could not be a main player for controlling background photochemistry in the troposphere and the stratosphere.

The very reactive nature of OH has hindered the development of reliable analytical techniques to quantify atmospheric OH concentrations. In the late 80s and early 90s, three different analytical techniques for measuring OH – long path-differential optical absorption spectrometry (LP-DOAS), laser induced fluorescence (LIF), and chemical ionization mass spectrometry (CIMS) – were developed and deployed on multiple platforms to test our understanding of tropospheric photochemistry (Heard and Pilling 2003). OH measurements by the LIF technique in high isoprene regions have consistently showed significant discrepancies from model predicted OH (Tan et al., 2001; Lelieveld et al., 2008; Hofzumahaus et al., 2009; and Whalley et al., 2011). Tan et al. (2001) reported OH and HO_2 measurements in a mixed northern hardwood forest (the PROPHET tower laboratory, Pellston, MI USA). This site has a moderate level of NO (100–200 pptv) and high isoprene concentrations (a few ppbv) during the daytime. A highly constrained photochemical box model of OH significantly underestimated the observed OH level (∼2.7 times). On the other hand, the model HO_2 results agreed well with the observed HO_2. This analysis led the authors to conclude that the recycling process from HO_2 to OH is poorly understood. These findings are consistent with recent results in two very different photochemical regimes. Lelieveld et al. (2008) presented airborne OH, HO_2 and other trace gas measurements over the pristine rain forest region of Surinam ($NO < 50$ pptv). Based on measured precursors, they simulated OH and HO_2 concentrations using a state of the art tropospheric chemistry model. Model results indicated significant underestimation of OH and reasonable prediction of HO_2. The authors hypothesized that unknown peroxy radical recycling processes from reactions of HO_2 with isoprene peroxy radicals may be the sources for the excess OH. During the Oxidant and Particle Photochemical Processes (OP-3) field campaign in a Borneo rain forest (another high isoprene-low NO region), investigators reported higher than expected OH levels that cannot be explained by conventional OH production and recycling rates (Whalley et al., 2011). Similar findings were also reported in a region with high isoprene concentrations that however is moderately polluted (a few hundreds pptv of NO), the Pearl River Delta area Hofzumahaus et al., 2009; Lu et al., 2012). Generally, it is proposed that unknown recycling processes from HO_2 to OH cause unexplained high levels of OH. Due to much higher concentrations of HO_2 in the atmosphere, relatively small recycling rate changes can significantly impact ambient OH levels. Additional primary radical sources (e.g. from photolysis of oxidized VOC) have also been invoked to explain the "missing OH" in some studies (Stavrakou et al., 2010).

Measured chemical loss rates of OH have also been employed as a metric to test our understanding of radical-driven photochemistry. Measurements of the chemical OH loss rate, otherwise known as OH reactivity (the reciprocal of lifetime of OH, s^{-1}), have been conducted in many different photochemical environments during the past decade. Lou et al. (2010) summarized published OH reactivity measurement datasets in major photochemical environments (urban, oceanic, and forest environments). The ratios of measured and calculated OH reactivity vary from 1–3. A ratio of one indicates that reactive trace gas measurements account for most of the reactive species in the atmosphere. On the other hand, higher ratios can be interpreted as the presence of unknown or unmeasured reactive trace gas species in the atmosphere. Ratios higher than one have mostly been reported in places where BVOCs play a major role in local photochemistry. More recent studies in a Northern European boreal forest reported much higher ratios of measured and calculated OH reactivity (up to ∼10; Sinha et al., 2010 and Noelscher et al., 2012). To explain the seemingly contradictory findings of missing OH sinks and sources, it has been suggested that reactions between OH, ozone and BVOCs can produce OH with significant yields (e.g. Tan et al., 2001 and Lelieveld et al., 2008)

Table 1. A summary of the instrument suite for BEACHON-ROCS 2010.

Measurement Items	Measurement Techniques	Measurement Uncertainty	References/Manufacturers
J_{NO_2}	Filter Radiometer	6 %	Metcon INC. Junkermann et al. (1989) and Volz-Thomas et al. (1996)
VOCs and OVOCs	Proton Transfer Reaction-Time of Flight-Mass Spectrometry and Proton Transfer Reaction-Quadrupole-Mass Spectrometry	15 %	Ionicon Analytik de Gouw and Warneke (2007) and Graus et al. (2010)
PAN and PPN	Chemical Ionization Mass Spectrometry	20 %	Slusher et al. (2004)
VOCs and OVOCs	Total Organic Gas Analyzer (in situ GC)	15 %	Apel et al. (2002)
Glyoxal and Formaldehyde	Laser Induced Florescence/Laser Induced Phosphorescence	20 %	di Gangi et al. (2011), Hottle et al. (2009) and Huisman et al. (2008)
OH Reactivity	Laser Induced Florescence	5 %	Sadanaga et al. (2004)
OH and H_2SO_4	Chemical Ionization Mass Spectrometry	35 %	Tanner et al. (1997) and Mauldin et al. (2010)
HO_2 and RO_2	Chemical Ionization Mass Spectrometry	35 %	Edwards et al. (2003) and Hornbrook et al. (2011)
*CO	Spectroscopic (IR)	15 %	Thermo Scientific Model 48i
NO/NO_2	Spectroscopic (Flourescence)	15 %	Eco Physics CLD 88 p
O_3	Spectroscopic (U.V.)	2 %	2B Technology

* The background drift was checked with CO-scrubbed air in every 10 min.

This paper presents comprehensive measurements to constrain HO_2 to OH recycling rates during the BEACHON-ROCS field campaign (August 2010). The main objective of the BEACHON-ROCS field campaign was to obtain comprehensive atmospheric measurements to constrain the OH sink, source and recycling terms in a ponderosa pine forest in the Colorado Rocky Mountains. The comprehensive measurement suite was used to constrain steady-state calculations and box model calculations using the Master Chemical Mechanism (Jenkin et al., 1997; Saunders et al., 2003). We systematically compare the modeling results with observations to improve the current understanding of radical photochemistry driven by BVOC oxidation.

2 Methods

2.1 Sampling site description

The Manitou Forest Observatory (MFO) in the U.S. Forest Service Manitou Experimental Forest near Woodland Park, Colorado U.S.A. (latitude 39°6′0″ longitude 105°5′30″ and elevation 2286 m) is situated in a ponderosa pine woodland in the Southern Colorado Rocky Mountain Front Range. The MFO is dominated by ponderosa pine trees that primarily emit 2-methyl-3-butene-2-ol (MBO) and monoterpenes (MT); isoprene and its oxidation products have been detected at relatively low concentrations since the inter-annual observations were initiated in 2009 (Kim et al., 2010). Therefore, uncertainties in isoprene-OH reaction mechanisms are considered relatively unimportant at this site (Archibald et al., 2010). The open pine woodland at the site has a Leaf Area Index (LAI) of about 3 m^2 m^{-2} for tree covered surfaces and a tree cover of about 60 % resulting in a landscape average LAI of about 1.9 m^2 m^{-2}. The average tree canopy height is ∼18 m. Major metropolitan areas near the MFO include Denver (∼85 km) and Colorado Springs (∼35 km) in the north eastern direction from the site, the origins of occasional pollution events at the research site. The dominant wind direction was either southwesterly (∼60 %) or northeasterly (∼40 %) (DiGangi et al., 2012). During the field observation, typical daytime high temperature was observed between 20 to 25 degree C and 5 to 10 degree C was observed for daytime low temperature. We did not include any data observed during the precipitation events.

Most atmospheric chemistry measurements at the site were conducted near the flux tower (∼30 meter height). An overview of the BEACHON-ROCS field campaign measurements is summarized in Table 1. In this paper, we only present the observational data under the canopy (1.6 m from the ground). Most of instrumentation listed in Table 1 shared a common inlet except, CO, OH, HO_2, RO_2, and OH reactivity that were measured at about the same height within a 20 m radius from the common inlet. The J_{NO_2} sensor was located on top of the OH inlet. More detailed experimental configurations will be presented in the BEACHON-ROCS overview paper (Karl et al., 2013).

2.2 OH, HO_2, and RO_2 measurements by Chemical Ionization Mass Spectrometry

OH was measured by chemical ionization mass spectrometry (CIMS) during the BEACHON-ROCS field campaign. The technique was developed by Eisele and Tanner (1991) and they have comprehensively discussed potential interferences and limitations of their initial design. In response to these limitations, Tanner et al. (1997) presented a modified instrument configuration to measure OH and H_2SO_4 as well as a calibration method, which is identical to the instrumentation for this study. This CIMS method uses NO_3^- for the reagent ion to selectively ionize sulfuric acid in an atmospheric pressure reaction chamber;

$$NO_3^-HNO_3(H_2O)_n + H_2SO_4 \rightarrow \quad \text{(R1)}$$
$$HSO_4^-(HNO_3)_mH_2O_p + HNO_3 + (H_2O)_r$$

where $m = 0$ or 1, n, p, and r are dependent upon water vapor concentrations

Before the ions are introduced into a detection chamber that consists of an octopole ion beam focus, quadrupole mass filter, and channeltron units, the ion clusters are dissociated in the collisional dissociation chamber (CDC) so that NO_3^- and HSO_4^- are the only ions to be quantified for monitoring ambient concentrations of H_2SO_4.

For OH measurement, ambient OH is chemically converted into $H_2^{34}SO_4$ before sample air is introduced into the ionization flow tube;

$$OH + {}^{34}SO_2 + M \rightarrow H^{34}SO_3 + M \quad \text{(R2)}$$
$$H^{34}SO_3 + O_2 \rightarrow {}^{34}SO_3 + HO_2 \quad \text{(R3)}$$
$${}^{34}SO_3 + H_2O + M \rightarrow H_2^{34}SO_4 + M \quad \text{(R4)}$$

By applying isotopically-labeled sulfur dioxide, we can separate ambient sulfuric acid from sulfuric acid produced by reaction with OH. Injections of ${}^{34}SO_2$ and propane, an OH scrubber for the background signal check, are controlled by two sets of front and rear injectors controlled by a VALCO (Houston, TX, USA) valve unit. The valve cycling period is typically set to 30 seconds.

Ambient OH and H_2SO_4 sensitivity to the CIMS system was calibrated using the scheme presented in Petaja et al. (2009). OH was generated by illuminating the sample air stream with a Hg-pen ray lamp immediately before the CIMS sampling tube (1/2″ stainless steel tubing). The photons from the lamp were filtered so that only 184.9 nm photons hit the water vapor in the sample air stream. The amount of photons from the UV lamp intensity was measured using a photomultiplier (R 5764, Hamamatsu Photonics K. K.). With the measured number of photons, the water vapor number density and the absorption cross-section at the given wavelength, OH concentrations from the photolysis were estimated. More detailed descriptions on the calibration procedure can be found in Petaja et al. (2009) and Sjostedt (2006). The estimated uncertainty for the OH measurement is 35 % and the lower limit of detection $\sim 4 \times 10^5$ molecules cm^{-3} for a 5-min average.

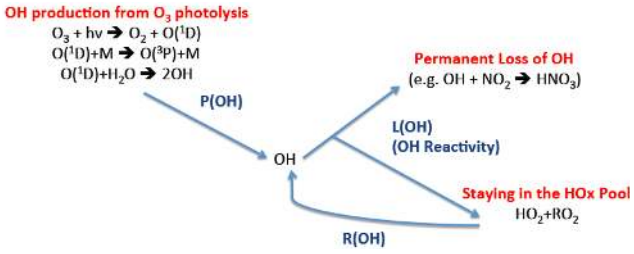

Fig. 1. Steady-state calculation scheme used in this study.

For HO_2 and RO_2 observations, the same ion chemistry as for OH quantification is applied. HO_2 and RO_2 are converted into OH by applying excess amounts of NO (0.3 % in volume) in the upstream of the sample flow. Since another research article on HO_2 and RO_2 observation and modeling results will be followed, in this paper we briefly introduce the principles of the HO_2 and RO_2 measurement technique, deployed for BEACHON campaign. Thorough descriptions on potential interferences and analytical characteristics can be found in Edwards et al. (2003) and Hornbrook et al. (2011). In addition, Mauldin et al. (2012) described potential interferences on background signals in OH quantifications using CIMS but we conducted frequent background characterization (every minute) to adequately subtract background signals.

2.3 Model calculations

2.3.1 Steady-state model

Highly constrained steady-state OH concentrations ($[OH]_{SS}$) were estimated based on the radical reaction scheme shown in Fig. 1. We conducted comprehensive measurements to constrain 1) OH production from ozone photolysis (ozone, H_2O concentrations and ozone photolysis rate (J_{O_3}) from NO_2 photolysis rate (J_{NO_2}) measurements) 2) OH chemical loss (OH reactivity measurement), and 3) OH recycling from HO_2 (HO_2 and NO measurements) as summarized in Table 1. The steady-state equation can be defined as follows;

$$d[OH]/dt = P(OH) + R(OH) - L(OH)[OH]_{SS} = 0 \quad (1)$$

where,

$$P(OH) = 2J_{O_3}k_7[H_2O][O_3]/(k_6[M])(\text{molecules cm}^{-3}\,\text{s}^{-1}) \quad (2)$$

From reactions

$$O_3 + hv \rightarrow O_2 + O(^1D),\ J_{O_3} \quad \text{(R5)}$$
$$O(^1D) + M \rightarrow O(^3P) + M,\ k_6 \quad \text{(R6)}$$
$$O(^1D) + H_2O \rightarrow 2OH,\ k_7 \quad \text{(R7)}$$

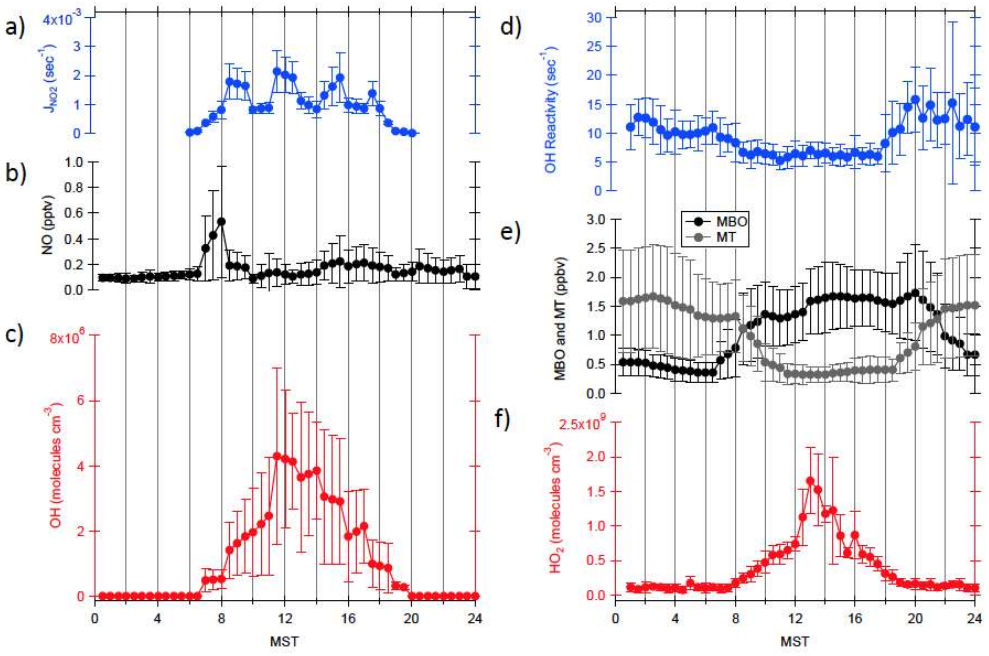

Fig. 2. Averaged diurnal cycles of **(a)** J_{NO_2}, **(b)** NO, **(c)** OH, **(d)** OH reactivity and **(e)** MBO and MT **(f)** HO_2 during the BEACHON-ROCS field campaign in August 2010.

L(OH) = OH reactivity (s^{-1}).

R(OH) = OH recycling rates (molecules cm^{-3} s^{-1}).

J_{O_3} was estimated from JNO_2 measurements by applying scaling factors from comparisons with theoretically calculated values using the scheme described by Saunders et al. (2003). As previously discussed, the underestimated recycling rates of OH from HO_2 and RO_2 have been proposed to be the major reason for unexpected high OH levels in isoprene rich regions. In this study, we consider only the conventional OH recycling pathway, which is the reaction of HO_2 with NO. Therefore, by comparing $[OH]_{SS}$ with measured OH concentrations ($[OH]_{MEA}$), we can assess whether additional recycling processes are needed to explain the measured levels of OH in a MBO and MT rich region. The uncertainty of $[OH]_{SS}$ assessed from the uncertainties of the input parameters is estimated ∼45 %.

2.3.2 0-D box model

Observationally-constrained chemical box model calculations were conducted using the University of Washington Chemical Box Model (UWCM). UWCM incorporates the Leeds Master Chemical Mechanism (MCM) v3.2 (Jenkin et al., 1997; Saunders et al., 2003) into a MATLAB-based source code (Wolfe and Thornton, 2011). The model was constrained with 60-min averaged observations. Utilized meteorological observations include temperature, pressure and relative humidity. NO_2 photolysis frequencies measured adjacent to the OH inlet were used to correct MCM-calculated photolysis frequencies for cloud and canopy cover. Chemical observations include OH, HO_2, CO, O_3, NO, NO_2, MBO, isoprene, monoterpenes (α-pinene, β-pinene, limonene, camphene and unspeciated monoterpenes), butadiene, benzene, toluene, oxygenated VOC (formaldehyde, glyoxal, acetone, methanol, acetaldehyde, methyl vinyl ketone, methacrolein, propanal, butanal), PAN and PPN. BEACHON included VOC observations from four different instruments measuring at varying heights with different reporting intervals (Kaser et al., 2012). For the present study, we utilize observations made by the Innsbruck PTR-TOF and the NCAR TOGA instruments at 23 m. To account for vertical gradients in emitted species, MBO and MT observations are scaled from 23 m to 4 m using VOC gradient measurements from the NCAR PTR-Quadrupole instrument. Data were averaged to a 60-min diurnal cycle for 17–20 August, except for NO_2 and TOGA observations. Insufficient coverage for these species required averaging over the entire dataset (1–31 August). Sensitivity tests were conducted to ensure that data averaging procedures do not affect our conclusions. CH_4 and H_2 concentrations were held constant at 1770 and 550 ppbv, respectively.

Several reactions in MCM v3.2 were updated as described in Wolfe and Thornton (2011). For monoterpenes, the explicit MCM mechanisms were used for α-pinene, β-pinene and limonene and the reaction scheme of Wolfe and Thornton (2011) was used for camphene. Unspeciated monoterpenes were treated similar to the unspeciated sesquiterpenes described in Wolfe and Thornton (2011) but with rate constants taken from the β-pinene mechanism. Sensitivity tests

indicate that newly-proposed isoprene peroxy radical isomerization chemistry (Crounse et al., 2011; Peeters and Müller, 2010; Peeters et al., 2009; Wolfe et al., 2012) influences modeled HO_x concentrations by less than 10 % for the conditions of this study. Given the comprehensive suite of constraints, emission and deposition were not considered explicitly, but an additional lifetime of 24 hours was given to all species to avoid the buildup of long-lived products.

The model was initialized at midnight and integrated for two days. Constraints were updated with observations every 60 min. The first day was treated as a "spin-up" day to allow secondary products to accumulate, and results are shown here for the second day. This model setup was sufficient to reproduce observed daytime OH reactivity to within 20 %, though we caution that a significant fraction of the modeled OH reactivity (∼40 %) is ascribed to unmeasured oxidized VOC. Results are shown for three scenarios: a base case where OH and HO_2 were not constrained to observations, and two scenarios where either OH or HO_2 were constrained.

3 Results and discussion

3.1 Observed parameters

The diurnal cycles of OH, HO_2, NO, J_{NO_2}, BVOC concentrations (MBO and MT) and OH reactivity during the BEACHON-ROCS field campaign are shown in Fig. 2. The OH and HO_2 CIMS inlets (about 3 m above the ground) were located under the tree canopy. J_{O_3} was calculated from J_{NO_2}, for which the sensor was located right above the HO_x inlets, and Fig. 2 shows that sporadic shade resulted in intermittent low, local primary production rates of OH. These low primary OH production rates are not reflected in the observed OH and HO_2 diurnal cycles, which show a regular diurnal cycle with daytime highs around 12:00 to 14:00. The observations remind us that radical concentrations are not solely governed by solar radiation at the exact location of the measurement instrumentation.

However, the importance of solar radiation for initiating radical chemistry is demonstrated by observations that OH was below the detection limit (5×10^5 molecules cm^{-3}) in the nighttime. The very low nighttime OH concentrations are contrary to previous reports of high nighttime OH levels at a mixed northern hardwood forest (University of Michigan Biological Station, Pellston, MI, USA) by Tan et al. (2001). The study reported that nighttime OH levels were ∼50 % of daytime maximum OH levels and speculated that Criegee radicals from the ozonolysis of MT could generate nighttime OH. Considering fairly high concentrations of MT (∼1.2 ppbv) at MFO during the night, the nighttime observations during BEACHON-ROCS appear to contradict these previous findings, though it is possible that the mechanism for nocturnal OH generation is highly dependent on the VOC mixture at a particular location. However, in a South Eastern Asian rain forest, the observed nighttime OH levels were also substantially lower (∼10 % or less than daytime peak OH levels; Whalley et al., 2011) than in the study of Tan et al. (2001).

The observed daytime OH concentrations during BEACHON-ROCS are similar to previously reported levels in rural forest environments (∼4×10^6 molecules cm^{-3}, Tan et al., 2001 and Carslaw et al., 2001). On the other hand, the observed daytime HO_2 level during this study is significantly higher (∼twice) than the HO_2 level observed during these studies. The variability of HO_2 concentrations in various environments has not been discussed as much as the variability of OH. This may be because in most cases, measured HO_2 showed much better agreement with model estimates than does OH (e.g. Tan et al., 2001). Any variability of HO_2 needs to be examined to assess the recycling source of OH from HO_2. NO, an important reducing agent for HO_2, was detected at slightly higher than 100 pptv during the daytime, which is higher than the nominal detection limit of ∼60 pptv. NO concentrations are much higher than those observed in the remote environments, where the higher than expected OH levels were observed (Lelieveld et al., 2008; Whalley et al., 2011). However, even at such moderate NO levels, models have been shown to under-predict observed OH concentrations by factors of 2–4 in high-isoprene conditions (Pearl River Delta, China and Pellston, Michigan; Lu et al., 2012).

The average measured OH reactivity (Fig. 2) is ∼6 sec^{-1} during the day and ∼10 sec^{-1} at night. Reactive gas measurements indicate that BVOCs, mostly MT (∼ 0.5 ppbv during daytime and ∼1.2 ppbv during nighttime) and MBO (∼1.6 ppbv during daytime and ∼0.6 ppbv an average for 10 a.m. to 2 p.m. and 9 p.m. to midnight, respectively), are the dominant OH sinks inside the forest canopy. The most dominant MT species, observed during the field campaign was β-pinene (35.2 %) followed by 3-carene (23.0 %), α-pinene (20.9 %) and limonene (17.5 %). More thorough discussion on VOC observations during the BEACHON-ROCS campaign will be submitted in the same ACP special issue (Kaiser et al., 2013). Contributions of isoprene to OH reactivity were minor. Isoprene concentrations at the site were relatively low during the BEACHON-ROCS campaign as previously reported (e.g. 0.3 ppbv maximum, 0.1 ppbv on average; Kim et al., 2010). The observed OH reactivity is comparable to previous measurements in the rural US but significantly lower than values observed in megacities and tropical rain forests (Lou et al., 2010). The observed daytime OH reactivity level during the BEACHON-ROCS campaign was the similar level to that observed in a Northern European boreal environment without any significant environmental perturbation where MT is the most dominant OH sink (Sinha et al., 2010; Noelscher et al., 2012). A more detailed analysis of OH reactivity and comparison with observed BVOCs at this site will be described in a separate publication (Nakashima et al., 2013).

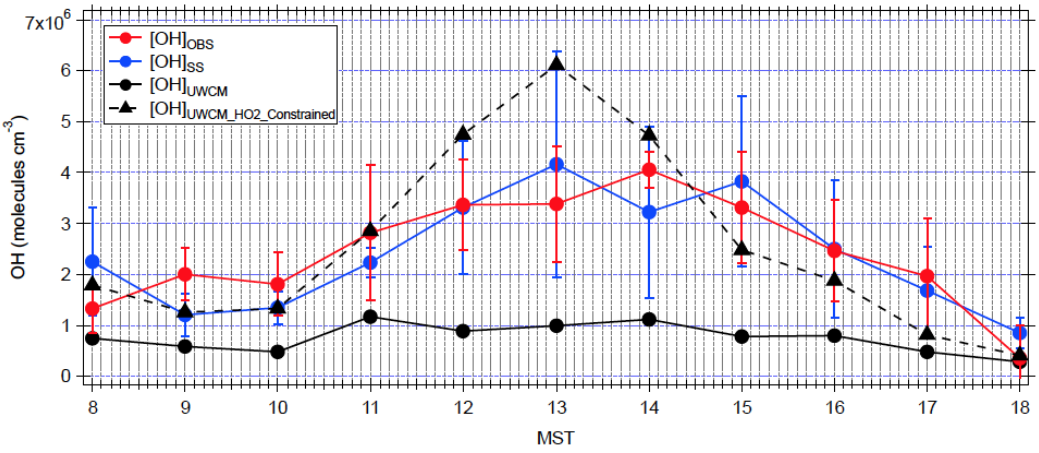

Fig. 3. Averaged diurnal cycles of observed OH ($[OH]_{MEA}$), steady-state model calculated ($[OH]_{SS}$), UWCM model calculated OH ($[OH]_{UWCM}$), and HO_2 constrained UWCM model calculated OH ($[OH]_{UWCM\_HO_2\_Constrained}$) for 16 to 19 August 2010.

3.2 Steady-state model calculations

A four-day period during the study provided a comprehensive dataset including all required measurements for the steady-state calculation (16 to 19 August). Similar diurnal cycles in all input parameters were observed over the four-day period. The averaged daily variations of $[OH]_{MEA}$ and $[OH]_{SS}$ for those four days are shown in Fig. 3. The error bars indicate one standard deviation for the averaged values. The $[OH]_{SS}$ shown in Fig. 3 captures both the magnitude and daily variation of $[OH]_{MEA}$ very well. The disagreement for the early morning is likely due to photolysis of HONO, which was not constrained in the steady-state calculation. High NO concentrations in the early morning have been observed for previous field studies in forested environments and may be explained by soil NO_x emissions and the boundary layer evolution, although local pollution sources are also a possibility (e.g. Alaghmand et al., 2011). The 1:1 plot between $[OH]_{MEA}$ and $[OH]_{SS}$ for the four comparison days (10 min average data) is presented in Fig. 4. Although the linear regression analysis has a slope that agrees with the 1:1 line within the uncertainties of measurement and calculations, a high degree of scatter is noticeable which may be explained by significant uncertainties from measurements used for $[OH]_{SS}$ (~50 %) as indicated by error bars obtained from the regression.

The excellent agreement of $[OH]_{MEA}$ and $[OH]_{SS}$ during this study is contrary to the previous studies in isoprene rich environments. These studies have consistently reported high unexplained levels of OH. To explore this issue further, the averaged daily variations of OH production rates from ozone photolysis and OH recycling from the HO_2 reaction with NO are presented in Fig. 5. In addition, the diurnal cycle in the ratio of OH production rate from HO_2 recycling to the OH production rate from ozone photolysis is also shown. The photolysis production rates observed during

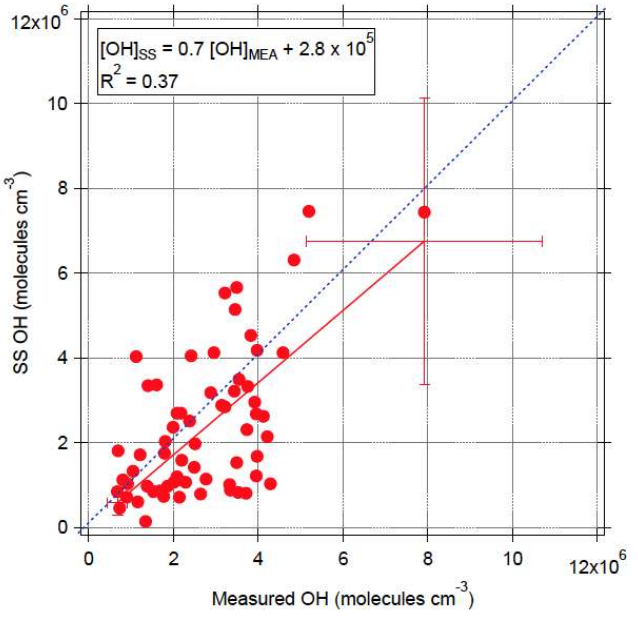

Fig. 4. A correlation plot with $[OH]_{MEA}$ and $[OH]_{SS}$ (red circles) and a 1:1 line (dashed line). The error bars on the regression line (red) represent uncertainties of $[OH]_{MEA}$ and $[OH]_{SS}$.

the BEACHON-ROCS campaign are about 30 % of the production rates observed during the PROPHET-1998 campaign (Tan et al., 2001), where the OH sensor was located above the forest canopy without shading from branches. Considering the attenuated J_{O_3} due to shade and cloud events during this study (Fig. 2), this difference is not surprising. As previously discussed, higher HO_2 levels (~4 times) in this study resulted in significantly higher OH production rates from recycling (~4 times) than those observed at PROPHET-1999 under similar NO_x conditions ($\sim 5 \times 10^6$ molecules cm^{-3} s^{-1} vs. $\sim 2 \times 10^7$ molecules cm^{-3} s^{-1}). Therefore, we can neglect

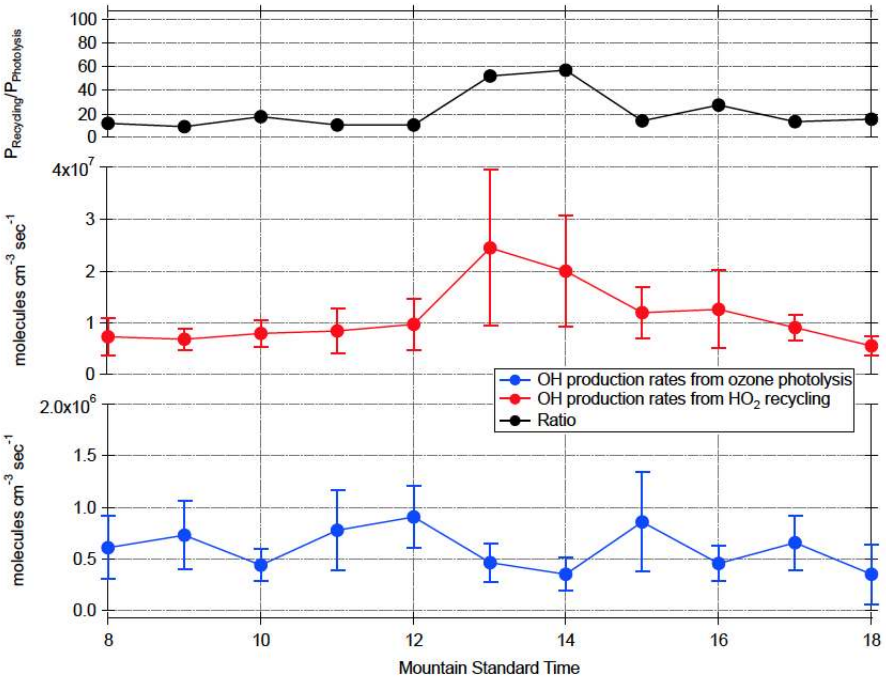

Fig. 5. Averaged diurnal cycles of OH photolysis production rates (blue), OH recycling rates (HO_2+NO, red) and their ratios (black) during the BEACHON-ROCS field campaign.

the photolytic production term in the steady state equation which gives;

$$R(OH) = L(OH)[OH] \quad (3)$$

$$[OH] = R(OH)/L(OH) \quad (4)$$

where, L(OH) = OH reactivity (s^{-1}), R(OH) = OH recycling rate = k_{HO_2+NO} $[HO_2][NO]$ (molecules cm^{-3} s^{-1})

This simplified equation provides the important insight that uncertainties in OH reactivity and OH recycling rates directly affect the accuracy of estimates of OH concentration. Measured OH reactivity values in forest environments are significantly higher than expected from measured trace gases. The ratios of measured to calculated OH reactivity have been reported to range from 1 up to 10 (Lou et al., 2010; Sinha et al., 2010; Noelscher et al., 2012). Therefore, if the steady-state equation was constrained by trace gas measurements, instead of directly by OH reactivity measurements, then $[OH]_{SS}$ would have been overestimated by a factor of 1 to 10. In addition, any uncertainty in the OH recycling rates linearly propagates to estimated $[OH]_{SS}$. These two independent sources of potential uncertainty can either cause an over- or underestimation of $[OH]_{SS}$ or result in reasonable predictions of ambient OH levels for the wrong reason. Only a comprehensive measurement suite can enable precise and accurate estimation of ambient OH concentrations. For example, a preliminary data analysis indicates that ~50 % of measured OH reactivity cannot be explained by the suite of VOC measurements (Nakashima et al., 2011). Therefore, the steady-state calculations without OH reactivity measurements would cause overestimation of OH by a factor of two.

3.3 UWCM model calculations

The predicted diurnal cycle in OH and HO_2 using the UWCM model scheme ($[OH]_{UWCM}$) is presented in Figs. 3 and 6. In the base scenario (both OH and HO_2 unconstrained), The UWCM significantly underestimates both OH and HO_2 (by as much as a factor of 8) during the BEACHON-ROCS field campaign. Since the steady state analysis indicates that HO_2 recycling is the main source for OH radicals, it is reasonable to hypothesize that the underprediction in OH is primarily due to the under-predicted HO_2. Indeed, constraining the model with measured HO_2 improves model-measurement agreement in the OH diurnal variations ($[OH]_{UWCM\_HO_2\_Constrained}$ in Fig. 3 by increasing OH concentrations during the daytime up to a factor of 6. Conversely, if the model is constrained to measured OH, modeled HO_2 concentrations only increase by a factor of ~2 ($[HO_2]_{UWCM\ OH\_Constrained}$ in Fig. 6). As shown in Fig. 7, the model calculated OH reactivity in the difference constraining scenarios agrees with the observed values within 20 %. Therefore, the chemical lifetime of OH is well constrained in each applied model scenario considering significant variations in OH and HO_2 levels in each model scenario. The reason for the higher predicted OH reactivity levels, when HO_2 is constrained, probably results in excess formation of OVOCs due to the higher predicted OH levels (Fig. 3).

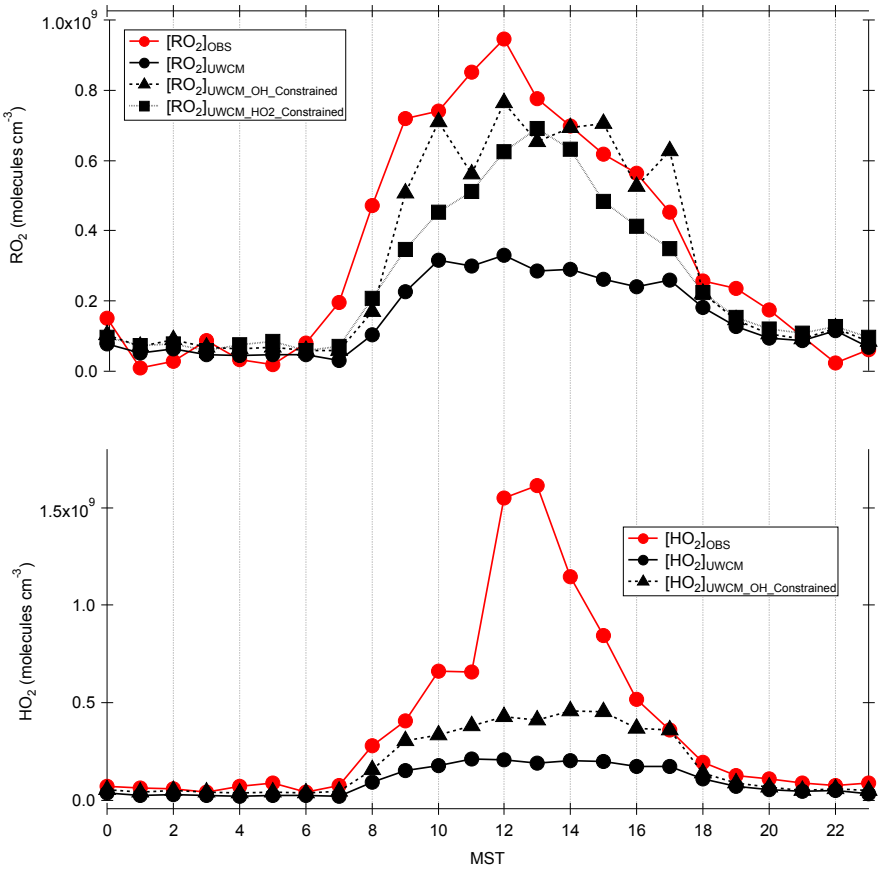

Fig. 6. The averaged diurnal cycles of $[HO_2]_{MEA}$, $[HO_2]_{UWCM}$, and $[HO_2]_{UWCM\_OH\_Constrained}$ in the bottom panel and $[RO_2]_{MEA}$, $[RO_2]_{UWCM}$, and $[RO_2]_{UWCM\_OH\_Constrained}$ during the BEACHON-ROCS field campaign.

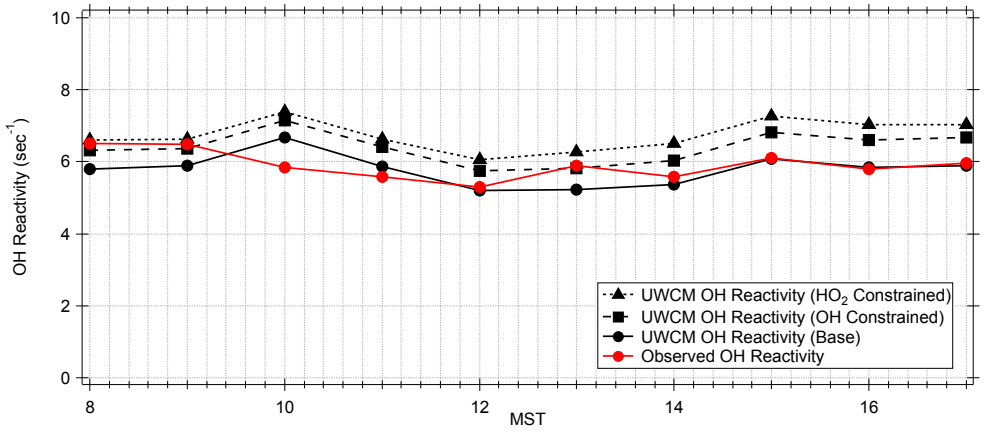

Fig. 7. The daytime variations of observed OH reactivity and UWCM calculated OH reactivity from the various model scenarios, described in the text.

Together, these results imply a source of HO_2 that is not currently represented in the model. Our model results suggest a missing HO_2 production rate of 1–7 ppbv h^{-1}, which is 2–3 times larger than total HO_2 production from the known tropospheric photochemical processes as shown in Fig. 8. The figure shows specific HO_2 chemical sources and sinks in the HO_2 constrained UWCM calculations. The black solid line (L-P) in Fig. 8 indicates the required HO_2 production rates to reconcile observed HO_2 concentrations, which cannot be explained by the currently known sources of HO_2. Potential

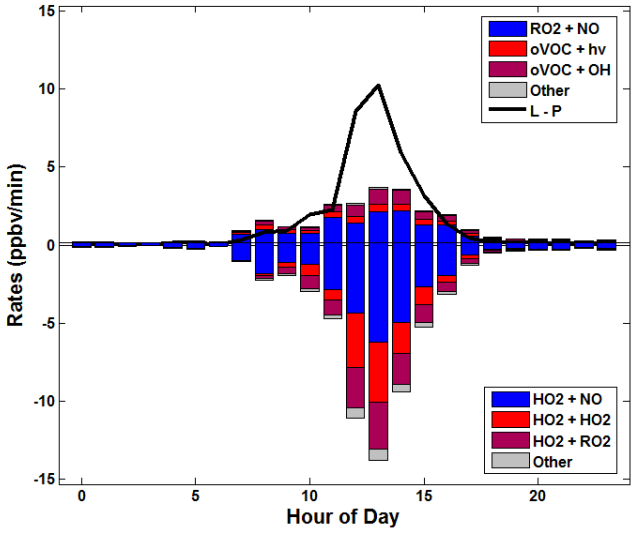

Fig. 8. UWCM model calculated HO_2 loss and production rates in different photochemical pathways (indicated as the colored bars). The black solid line (overall loss rate – overall production rates; L-P) shows required production rates to resolve the observed unexplained higher HO_2 level.

explanations for this missing source include (1) Transport of HO_2 from more highly irradiated regions within or above the canopy, (2) photolysis of oxidized VOC or other species that are not included in the model, or (3) additional reactions of RO_2 with unidentified reducing agents (e.g. Hofzumahaus et al., 2009). First, it is possible that the photolysis rates, scaled by the measured J_{NO_2} (Fig. 2), are not an accurate representation of the "average" canopy environment. This is a reasonable hypothesis, since the chemical lifetime of HO_2 (∼100 secs) is on the order of the timescale for canopy mixing/venting, so HO_2 can be transported from sunny to shady areas under the forest canopy. Running the model under a full sun scenario (i.e. no photolysis attenuation) increases modeled HO_2 concentrations by a factor of 2 – not enough to explain observed HO_2 concentrations. If the entirety of the missing HO_2 source is due to photolysis of unknown BVOCs, the HO_2 production rate would need to be ∼ 100 times that from HCHO photolysis. Given that the modeled OH reactivity is within 30 % of observations (Nakashima et al., 2012), this seems unlikely. Still, it is possible that yet-unidentified VOC degradation chemistry produces oxidized VOC that, by virtue of a short lifetime with respect to photolysis, do not build up to appreciable concentrations and thus do not contribute significantly to OH reactivity. Such compounds could also be directly emitted from the biosphere. This hypothesis would also be consistent with observations of anomalously high HCHO fluxes during the same campaign (DiGangi et al., 2011). Finally, modeled HO_2 production stems primarily from reaction of NO with RO_2 under the conditions of the current study, thus it might be possible to generate additional HO_2 by augmenting this chemistry. Indeed, modeled total peroxy radical concentrations (RO_2) agree moderately well with observations in the model run with OH constrained as shown in Fig. 6, suggesting issues in the partitioning of peroxy radicals. Implementing a scheme to convert RO_2 to HO_2 and HO_2 to OH with an artificial reducing agent, as suggested by Hofzumahaus et al. (2009), effectively increases OH concentrations without affecting HO_2. At present, however, we cannot account for the missing source of HO_2. We are preparing a follow-up publication to specifically examine partitioning between RO_2 and HO_2 in a MBO dominant photochemical environment. It should be also noted that potential interferences in LIF techniques in OH quantifications from background quantification processes (Mao et al., 2012) and HO_2 quantifications from RO_2 radical (Fuchs et al., 2011). However, these reports on potential interferences have not been consistent from multiple studies. For example, a few recent studies about intercomparison between LIF techniques with DOAS and CIMS techniques reported excellent agreements between the techniques (Fuchs et al., 2012; Ren et al., 2011). One should also note that Hornbrook et al. (2011) indicated potential interferences in HO_2 quantifications from RO_2 from chemical conversion processes in the CIMS application for HO_2 and RO_2 quantifications.

These results suggest a need to rethink the oxidation capacity in the troposphere, especially in BVOC-dominated regions. As soon as an extremely short-lived species such as OH reacts with reactive BVOCs, it produces one or multiple HO_x (OH, HO_2, or RO_2). Therefore, the capacity of the oxidant pool (HO_x) is maintained or even magnified through BVOC oxidation reactions. The oxidant pool, including OH, HO_2 and RO_2, has a long enough lifetime (∼100 s) to be transported at the canopy scale (potentially even larger scales). The ratios of OH to HO_2 are determined by the surrounding photochemical environment such as concentrations of NO or other potential reducing agents as hypothesized in recent publications (e.g. Hofzumahaus et al., 2009). This perspective is summarized in Fig. 9. The inability of an up-to-date near explicit chemical scheme to correctly reproduce the observed size of the oxidant pool propagates directly into estimates of oxidizing capacity inside of the canopy, which is mostly determined by OH concentrations. On the other hand, the present measurement dataset from MFO shows that constraining both the main component of the oxidant pool (mostly HO_2) and oxidant-trace gas interaction (OH reactivity) is sufficient to predict OH concentrations in this environment. Moreover, at MFO NO radical is sufficient to explain observed recycling rates. This finding strongly suggests that BVOCs other than isoprene, such as MBO and monoterpenes, do not cause an amplification of the oxidation capacity that have been reported in environments with high isoprene and comparable NO levels (Tan et al., 2001; Hofzumahaus et al., 2009; Lu et al., 2012). However, one should note that unknown HO_2 sources are appeared to amplify oxidation capacity in this environment.

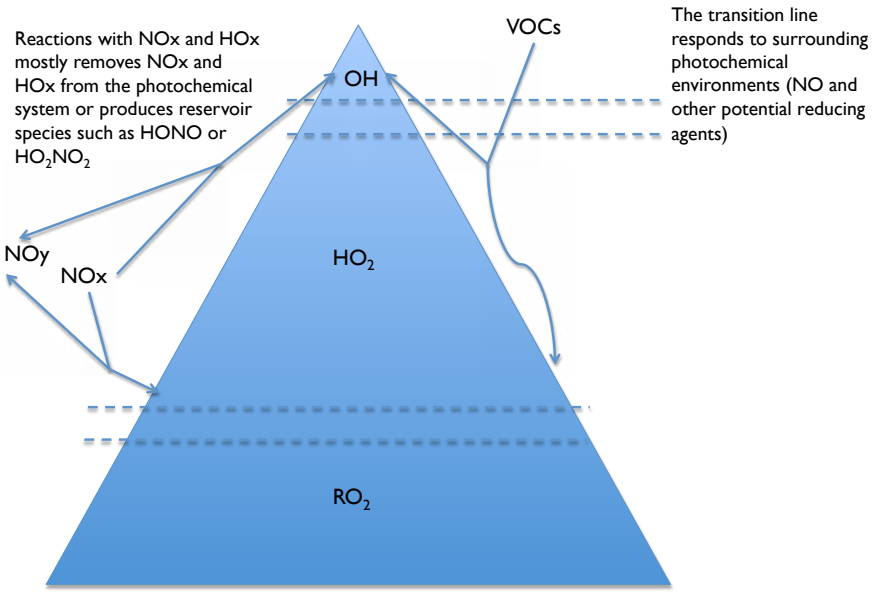

Fig. 9. Tropospheric interactions of oxidant pool NO_x-NO_y-VOCs (NO_y, reactive oxidized nitrogen). VOC oxidation by OH redistributes within the oxidant pool but does not change the size of the pool.

4 Summary

During the BEACHON-ROCS field campaign, a comprehensive measurement suite was deployed to constrain photolytic production, chemical loss and recycling of OH. The results were used to evaluate our current understanding of HO_x radical-BVOC (mostly, MBO and MT) interactions by comparing measured OH and model calculated OH using highly constrained steady-state ($[OH]_{SS}$) and explicit box model ($[OH]_{UWCM}$) calculations. $[OH]_{SS}$ shows an excellent agreement with $[OH]_{MEA}$. Further analysis of photolysis production rates from ozone photolysis and recycling rates (HO_2+NO) of OH indicate that the recycling production of OH is ∼20 times higher than the photolysis production. Thus, in the canopy environment, $[OH]_{SS}$ is primarily controlled by the HO_x recycling rate and total OH reactivity. Observational constraints on both OH sources and sinks provides a means to assess the magnitude of additional unknown OH production channels, which have been reported for isoprene-dominated environments with similar NO levels (Lu et al., 2012). Our results indicate that the conventional recycling pathway (HO_2+NO) is dominant in a non-isoprene forest environment. In contrast, $[OH]_{UWCM}$ shows very poor agreement with $[OH]_{MEA}$. Once HO_2 in the UWCM model calculations is constrained by $[HO_2]_{MEA}$, $[OH]_{UWCM\_HO_2\text{-}Constrained}$ is in better agreement with $[OH]_{MEA}$. Further model analysis suggests an unidentified source of HO_2 that may be due to photolysis of oxidized VOC or reactions of RO_2. Therefore, a simple box-model scheme may not accurately describe HO_2 distributions inside of forest canopies and this uncertainty propagates directly into OH estimations. This discussion highlights the importance of accurate measured constraints on the relatively long-lived oxidant pool (HO_2 and RO_2) and recycling processes such as reaction of HO_2 with reducing agents (e.g. NO) and HO_2-RO_2 reaction mechanisms. Finally, as Atkinson (2000) claimed, more careful laboratory characterization of reaction kinetics of RO_2 + NO is required considering kinetic information about RO_2 + NO has been deduced from experiments with alkane originated proxy radicals.

Acknowledgements. The National Center for Atmospheric Research is operated by the University Corporation for Atmospheric Research under sponsorship from the US National Science Foundation. Any opinions, findings and conclusions or recommendations expressed in this publication are those of the authors and do not necessarily reflect the views of the National Science Foundation. The authors also thank the National Science Foundation (ATM 0852406) and the Austrian Science Fund (FWF): [L518]. Lisa Kaser is a recipient of a DOC-fFORTE-fellowship of the Austrian Academy of Sciences at the Institute of Ion Physics and Applied Physics. GMW acknowledges support from the NOAA Climate and Global Change Postdoctoral Fellowship Program. Finally, we thank the US Forest Service, specifically Richard Oakes, for logical support.

Edited by: R. Holzinger

References

Alaghmand, M., Shepson, P. B., Starn, T. K., Jobson, B. T., Wallace, H. W., Carroll, M. A., Bertman, S. B., Lamb, B., Edburg, S. L., Zhou, X., Apel, E., Riemer, D., Stevens, P., and Keutsch, F.: The morning NOx maximum in the forest atmosphere boudary layer, Atmos. Chem. Phys. Discuss., 11, 29251–29282, doi:10.5194/acpd-11-29251-2011, 2011.

Apel, E. C., Riemer, D. D., Hills, A., Baugh, W., Orlando, J., Faloona, I., Tan, D., Brune, W., Lamb, B., Westberg, H., Carroll, M. A., Thornberry, T., and Geron, C. D.: Measurement and interpretation of isoprene fluxes and isoprene, methacrolein, and methyl vinyl ketone mixing ratios at the PROPHET site during the 1998 intensive, J. Geophys. Res.-Atmos., 107, 4034 doi10.1029/2000jd000225, 2002.

Archibald, A. T., Jenkin, M. E., and Shallcross, D. E.: An isoprene mechanism intercomparison, Atmos. Environ., 44, 5356–5364, doi:10.1016/j.atmosenv.2009.09.016, 2010.

Atkinson, R.: Atmospheric chemistry of VOCs and NO_x, Atmos. Environ., 34, 2063–2100, 2000.

Carslaw, N., Creasey, D. J., Harrison, D., Heard, D. E., Hunter, M. C., Jacobs, P. J., Jenkin, M. E., Lee, J. D., Lewis, A. C., Pilling, M. J., Saunders, S. M., and Seakins, P. W.: OH and HO_2 radical chemistry in a forested region of north-western Greece, Atmos. Environ., 35, 4725–4737, doi:10.1016/s1352-2310(01)00089-9, 2001.

Chameides, W. L. and Cicerone, R. J.: Effects of nonmethane hydrocarbons in atmosphere, J. Geophys. Res.-Ocean. Atmos., 83, 947–952, doi:10.1029/JC083iC02p00947, 1978.

Crounse, J. D., Paulot, F., Kjaergaard, H. G., and Wennberg, P. O.: Peroxy radical isomerization in the oxidation of isoprene, Phys. Chem. Chem. Phys., 13, 13607–13613, 2011.

Crutzen, P. J.: Photochemical reactions initiated by and influencing ozone in unpolluted tropospheric air, Tellus, 26, 47–57, 1974.

de Gouw, J. and Warneke, C.: Measurements of volatile organic compounds in the earths atmosphere using proton-transfer-reaction mass spectrometry, Mass Spectrom. Rev., 26, 223–257, 2007.

Di Gangi, J., Boyle, E. S., Karl, T., Turnipseed, A., Kim, S., Cantrell, C., Mauldin, R. L., Zheng, W., Flocke, F., Hall, S. R., Ullmann, K., Nakashima, Y., Paul, J. G., Wolfe, G. M., Desai, A. R., Kajii, Y., Guenther, A., and Keutsch, F.: First direct measurements of formaldehyde flux via eddy covariance: Implications for missing in-canopy formaldehyde sources, Atmos. Chem. Phys., 11, 10565–10578, doi:10.5194/acp-11-10565-2011, 2011.

DiGangi, J. P., Henry, S. B., Kammrath, A., Boyle, E. S., Kaser, L., Schnitzhofer, R., Graus, M., Turnipseed, A., Park, J.-H., Weber, R. J., Hornbrook, R., Cantrell, C., Maudlin, R. L., III, Kim, S., Nakashima, Y., Wolfe, G. M., Kajii, Y., Apel, E., Goldstein, A. H., Guenther, A., Karl, T., Hansel, A., and Keutsch, F. N.: Observations of glyoal and formaldehyde as metrics for the anthropogenic impact on rural photochemistry, Atmos. Chem. Phys., 12, 9529–5943, doi:10.5194/acp-12-9529-2012, 2012.

Edwards, G. D., Cantrell, C. A., Stephens, S., Hill, B., Goyea, O., Shetter, R. E., Mauldin, R. L., Kosciuch, E., Tanner, D. J., and Eisele, F. L.: Chemical ionization mass spectrometer instrument for the measurement of tropospheric HO_2 and RO_2, Analyt. Chem., 75, 5317–5327, 2003.

Eisele, F. L. and Tanner, D. J.: Ion-assisted tropospheric OH measurements, J. Geophys. Res.-Atmos., 96, 9295–9308, doi:10.1029/91jd00198, 1991.

Fuchs, H., Bohn, B., Hofzumahaus, A., Holland, F., Lu, K., Nehr, S., Rohrer, F., and Wahner, A.: Detection of HO_2 by laser-induced fluorescence: Calibration and interferences from RO_2 radicals, Atmos. Meas. Tech., 4, 1209–1225, doi:10.5194/amt-4-1209-2011, 2011.

Fuchs, H., Dorn, H.-P., Bachner, M., Bohn, B., Brauers, T., Gomm, S., Hofzumahaus, A., Holland, F., Nehr, S., Rohrer, F., Tillmann, R., and Wahner, A.: Comparison of oh concentration measurements by DOAS and LIF during SAPHIR chamber experiments at high OH reactivity and low NO concentrations, Atmos. Meas. Tech., 5, 1611–1626, doi:10.5194/amt-5-1611-2012, 2012.

Graus, M., Muller, M., and Hansel, A.: High resolution PTR-TOF: Quantification and formula confirmation of VOC in real time, J. Am. Soc. Mass Spectrom., 21, 1037–1044, 2010.

Heard, D. E. and Pilling, M. J.: Measurement of OH and HO_2 in the troposphere, Chem. Rev., 103, 5163–5198, doi:10.1021/cr020522s, 2003.

Hofzumahaus, A., Rohrer, F., Lu, K. D., Bohn, B., Brauers, T., Chang, C. C., Fuchs, H., Holland, F., Kita, K., Kondo, Y., Li, X., Lou, S. R., Shao, M., Zeng, L. M., Wahner, A., and Zhang, Y. H.: Amplified trace gas removal in the troposphere, Science, 324, 1702–1704, doi:10.1126/science.1164566, 2009.

Hornbrook, R. S., Crawford, J., Edwards, G. D., Goyea, O., Mauldin, R. L., Olson, J. S., and Cantrell, C. A.: Measurements of tropospheric HO_2 and RO_2 by oxygen dilution modulation and chemical ionization mass spectrometry, Atmos. Meas. Tech., 4, 735–756, doi:10.5194/amt-4-735-2011, 2011.

Huisman, A. J., Hottle, J. R., Coenes, K. L., Di Gangi, J. P., Galloway, M. M., Kammrath, A., and Keutsch, F. N.: Laser-induced phosphorescence for the in situ detection of glyoxal at part per trillion mixing ratios, Analyt. Chem., 80, 5584–5591, 2008.

Jenkin, M. E., Saunders, S. M., and Pilling, M. J.: The tropospheric degradation of volatile organic compounds: A protocol for mechanism development, Atmos. Environ.. 31, 81–104, doi:10.1016/s1352-2310(96)00105-7, 1997.

Jenkin, M. E., Saunders, S. M., and Pilling, M. J.: The tropospheric degradation of volatile organic compounds: A protocol for mechanism development, Atmos. Environ., 31, 81–104, 1997.

Junkermann, F., Platt, U., and Volz-Thomas, A.: A photoelectric detector for the measurement of photolysis frequencies of ozone and other atmospheric molecules, J. Atmos. Chem., 8, 203–227, 1989.

Kaser, L., Karl, T., Schnitzhofer, R., Graus, M., Herdlinger-Blatt, I. S., DiGangi, J. P., Sive, B., Turnipseed, A., Hornbrook, R. S., Zheng, W., Flocke, F. M., Guenther, A., Keutsch, F. N., Apel, E., and Hansel, A.: Comparison of different real time VOC measurement techniques in a ponderosa pine forest, Atmos. Chem. Phys. Discuss., 12, 27955–27988, doi:10.5194/acpd-12-27955-2012, 2012.

Kim, S., Karl, T., Guenther, A., Tyndall, G., Orlando, J., Harley, P., Rasmussen, R., and Apel, E.: Emissions and ambient distributions of biogenic volatile organic compounds (BVOCs) in a ponderosa pine ecosystem: Interpretation of PTR-MS mass spectra, Atmos. Chem. Phys., 10, 1759–1771, doi:10.5194/acp-10-1759-2010, 2010.

Lelieveld, J., Butler, T. M., Crowley, J. N., Dillon, T. J., Fischer, H., Ganzeveld, L., Harder, H., Lawrence, M. G., Martinez, M., Taraborrelli, D., and Williams, J.: Atmospheric oxidation

capacity sustained by a tropical forest, Nature, 452, 737–740, doi:10.1038/nature06870, 2008.

Levy, H.: Normal atmosphere – large radical and formaldehyde concentrations predicted, Science, 173, 141–143, doi:10.1126/science.173.3992.141, 1971.

Levy, H.: Photochemistry of lower troposphere, Planet Space Sci., 20, 919–935, doi:10.1016/0032-0633(72)90177-8, 1972.

Logan, J. A., Prather, M. J., Wofsy, S. C., and McElroy, M. B.: Tropospheric chemistry – a global perspective, J. Geophys. Res.-Ocean. Atmos., 86, 7210–7254, doi:10.1029/JC086iC08p07210, 1981.

Lou, S., Holland, F., Rohrer, F., Lu, K., Bohn, B., Brauers, T., Chang, C. C., Fuchs, H., Haseler, R., Kita, K., Kondo, Y., Li, X., Shao, M., Zeng, L., Wahner, A., Zhang, Y., Wang, W., and Hofzumahaus, A.: Atmospheric OH reactivities in the Pearl River Delta – China in summer 2006: Measurement and model results, Atmos. Chem. Phys., 10, 11243–11260, doi:10.5194/acp-10-11243-2010, 2010.

Lovelock, J. E.: Methyl chloroform in troposphere as an indicator of OH radical abundance, Nature, 267, 32–32, doi:10.1038/267032a0, 1977.

Lu, K. D., Rohrer, F., Holland, F., Fuchs, H., Bohn, B., Brauers, T., Chang, C. C., Haseler, R., Hu, M., Kita, K., Kondo, Y., Li, X., Lou, S. R., Nehr, S., Shao, M., Zeng, L. M., Wahner, A., Zhang, Y. H., and Hofzumahaus, A.: Observation and modelling of OH and HO_2 concentrations in the Pearl River Delta 2006: A missing oh source in a voc rich atmosphere, Atmos. Chem. Phys., 12, 1541–1569, doi:10.5194/acp-12-1541-2012, 2012.

Mao, J., Ren, X., Zhang, L., Van Duin, D. M., Cohen, R. C., Park, J.-H., Goldstein, A. H., Paulot, F., Beaver, M. R., Crounse, J. D., Wennberg, P. O., DiGangi, J. P., Henry, S. B., Keutsch, F. N., Park, C., Schade, G. W., Wolfe, G. M., Thornton, J. A., and Brune, W. H.: Insights into hydroxyl measurements and atmospheric oxidation in a california forest, Atmos. Chem. Phys., 12, 8009–8020, doi:10.5194/acp-12-8009-2012, 2012.

Mauldin, R. L., Berndt, T., Sipila, M., Paasonen, P., Petaja, T., Kim, S., Kurten, T., Stratmann, F., Kerminen, V. M., and Kulmala, M.: A new atmospherically relevant oxidant of sulphur dioxide, Nature, 488, 193–196, doi:10.1038/nature11278, 2012.

Mauldin, R. L., Kosciuch, E., Eisele, F. L., Huey, L. G., Tanner, D. J., Sjostedt, S. J., Blake, D., Chen, G., Crawford, J., and Davis, D.: South pole Antarctica observations and modeling results:New insights on HO_x radical and sulfur chemistry, Atmos. Environ., 44, 572–581, 2010.

Nakashima, Y., Ida, A., Kajii, Y., Greenberg, J., Karl, T., Kim, S., Turnipseed, A., Guenther, A., Di Ganigi, J., Henry, J., Keutsch, F., Schnitzhofer, R., Kaser, L., and Hansel, A.: Total OH reactivity measurements at manitou experimental forest in summer season during beachon-rocs field campaign, American Geophysical Union Fall Meeting, San Francisco, CA USA, 2011.

Nakashima, Y., Ida, A., Kajii, Y. J., Greenberg, J., Karl, T., Kim, S., Turnipseed, A., Guenther, A. B., DiGangi, J. P., Henry, S. B., Keutsch, F. N., Schnitzhofer, R., Kaser, L., and Hansel, A.: Total OH reactivity measurements at the Manitou Experimental Forest in summer season during BEACHON-ROCS campaign, Atmos. Chem. Phys., in preparation, 2013.

Nolscher, A. C., Williams, J., Sinha, V., Custer, T., Song, W., Johnson, A. M., Axinte, R., Bozem, H., Fischer, H., Pouvesle, N., Phillips, G., Crowley, J. N., Rantala, P., Rinne, J., Kulmala, M., Gonzales, D., Valverde-Canossa, J., Vogel, A., Hoffmann, T., Ouwesloot, H. G., Vila-Guerau de Arellano, J., and Lelieveld, J.: Summertime total oh reactivity measurements from boreal forst during HUMPPA-COPEC 2010, Atmos. Chem. Phys., 12, 8257–8270, doi:10.5194/acp-12-8257-2012, 2012.

Peeters, J. and Müller, J. F.: HO_x radical regeneration in isoprene oxidation via peroxy radical isomerisations. II: experimental evidence and global impact, Phys. Chem. Chem. Phys., 12, 14227–14235, 2010.

Peeters, J., Nguyen, T. L., and Vereecken, L.: HO_x radical regeneration in the oxidation of isoprene, Phys. Chem. Chem. Phys., 11, 5935–5939, 2009.

Petaja, T., Mauldin, R. L., Kosciuch, E., McGrath, J., Nieminen, T., Paasonen, P., Boy, M., Adamov, A., Kotiaho, T., and Kulmala, M.: Sulfuric acid and OH concentrations in a boreal forest site, Atmos. Chem. Phys., 9, 7435–7448, doi:10.5194/acp-9-7435-2009, 2009.

Ren, X., Mao, J., Brune, W., Cantrell, C., Maudlin, R. L., Hornbrook, R., Kosciuch, E., Olson, J. R., Crawford, J., Chen, G., and Singh, H. B.: Airbonre intercomparison of HO_x measurements using laser-induced fuorescence and chemical ionization mass spectrometer during ARCTAS, Atmos. Meas. Tech., 5, 2025–2037, doi:10.5194/gmd-5-2025-2012, 2012.

Sadanaga, Y., Yoshino, A., Watanabe, K., Yoshioka, A., Wakazono, Y., Kanaya, Y., and Kajii, Y.: Development of a measurement system of OH reactivity in the atmosphere by using a laser-induced pump and probe tehcnqiue, Rev. Sci. Instr., 75, 2648–2655, 2004.

Saunders, S. M., Jenkin, M. E., Derwent, R. G., and Pilling, M. J.: Protocol for the development of the Master Chemical Mechanism, MCM v3 (Part A): tropospheric degradation of non-aromatic volatile organic compounds, Atmos. Chem. Phys., 3, 161–180, doi:10.5194/acp-3-161-2003, 2003.

Sinha, V., Williams, J., Lelieveld, J., Ruuskanen, T. M., Kajos, M. J., Patokoski, J., Helllen, H., Hakola, H., Mogensen, D., Boy, M., Rinne, J., and Kulmala, M.: OH reactivity measurements within a Boreal Forest: Evidence for unknown reactive emissions, Environ. Sci. Technol., 44, 6614–6620, 2010.

Singh, H. B.: Atmospheric halocarbons - evidence in favor of reduced average hydroxyl radical concentration in troposphere, Geophys. Res. Lett., 4, 101–104, doi:10.1029/GL004i003p00101, 1977.

Sjostedt, S. J.: Investigation of photochemistry at high latitudes: Comparison of model predictions to measurements of short lived species, Ph. D., Earth and Atmospheric Sciences, Georgia Institute of Technology, Atlanta, USA, 174 pp., 2006.

Slusher, D. L., Huey, L. G., Tanner, D. J., Flocke, F., and Roberts, J. M.: A thermal dissociation-chemical ionization mass spectrometry (TD-CIMS) technique for the simultaneous measurement of peroxyacyl nitrates and dinitrogen pentoxide, J. Geophys. Res., 109, D19315, doi:10.1029/2004JD004670, 2004.

Stavrakou, T., Peeters, J., and Müller, J.-F.: Improved global modelling of HO_x recycling in isoprene oxidation: evaluation against the GABRIEL and INTEX-A aircraft campaign measurements, Atmos. Chem. Phys., 10, 9863–9878, doi:10.5194/acp-10-9863-2010, 2010.

Tan, D., Faloona, I., Simpas, J. B., Brune, W., Shepson, P. B., Couch, T. L., Sumner, A. L., Carroll, M. A., Thornberry, T., Apel, E., Riemer, D., and Stockwell, W.: HO_x budgets

in a deciduous forest: Results from the PROPHET summer 1998 campaign, J. Geophys. Res.-Atmos., 106, 24407–24427, doi:10.1029/2001jd900016, 2001.

Tanner, D. J., Jefferson, A., and Eisele, F. L.: Selected ion chemical ionization mass spectrometric measurement of OH, J. Geophys. Res.-Atmos., 102, 6415–6425, doi:10.1029/96jd03919, 1997.

Whalley, L. K., Edwards, P. M., Furneaux, K. L., Goddard, A., Ingham, T., Evans, M. J., Stone, D., Hopkins, J. R., Jones, C. E., Karunaharan, A., Lee, J. D., Lewis, A. C., Monks, P. S., Moller, S. J., and Heard, D. E.: Quantifying the magnitude of a missing hydroxyl radical source in a tropical rainforest, Atmos. Chem. Phys., 11, 7223–7233, doi:10.5194/acp-11-7223-2011, 2011.

Wofsy, S. C., McConnel, J. C., and McElroy, M. B.: Atmospheric CH_4, CO, and CO_2, J. Geophys. Res., 77, 4477–4493, doi:10.1029/JC077i024p04477, 1972.

Wolfe, G. M. and Thornton, J. A.: The Chemistry of Atmosphere-Forest Exchange (CAFE) Model – Part 1: Model description and characterization, Atmos. Chem. Phys., 11, 77–101, doi:10.5194/acp-11-77-2011, 2011.

Wolfe, G. M., Crounse, J. D., Parrish, J. D., St. Clair, J. M., Beaver, M. R., Paulot, F., Yoon, T. P., Wennberg, P. O., and Keutsch, F. N.: Photolysis, OH reactivity and ozone reactivity of a proxy for isoprene-derived hydroperoxyenals (HPALDs), Phys. Chem. Chem. Phys., 14, 7276–7286, doi:10.1039/C2CP40388A, 2012.